

Document downloaded from:

<http://hdl.handle.net/10251/59168>

This paper must be cited as:

Ferre Vilaplana, A. (2014). Oxidation mechanism of formic acid on the bismuth adatom-modified Pt(111) surface. *Journal of the American Chemical Society*. 13110-13113.



The final publication is available at

<http://dx.doi.org/10.1021/ja505943h>

Copyright American Chemical Society

Additional Information

Oxidation Mechanism of Formic Acid on the Bi-adatom Modified Pt(111) Surface.

Juan Victor Perales-Rondón[†], Adolfo Ferre-Vilaplana[‡], Juan M. Feliu[†] and Enrique Herrero^{†*}.

[†]Instituto de Electroquímica, Universidad de Alicante, Apdo. 99, E-03080 Alicante, Spain

[‡]Instituto Tecnológico de Informática, Ciudad Politécnica de la Innovación, Camino de Vera s/n, E-46022 Valencia, Spain, and Departamento de Sistemas Informáticos y Computación, Escuela Politécnica Superior de Alcoy, Universidad Politécnica de Valencia, Plaza Ferrándiz y Carbonell s/n, E-03801 Alcoy, Spain

Supporting Information Placeholder

ABSTRACT: In order to improve catalytic processes, elucidation of reaction mechanisms is essential. Here, supported by a combination of experimental and computational results, the oxidation mechanism of formic acid on Pt(111) electrodes modified by the incorporation of bismuth adatoms is revealed. In the proposed model, formic acid is first physisorbed, on bismuth, and then deprotonated and chemisorbed in formate form, also on bismuth, from which configuration the C-H bond is cleaved, on a neighbor Pt site, yielding CO₂. It was computationally found that the activation energy for the C-H bond cleavage step is negligible, which was also verified experimentally.

Cleaner energy based on the oxidation of small organic molecules (i.e., formic acid, methanol, ethanol ...) in fuel cells requires efficient electrocatalysts capable of operating at low overpotentials and high current densities. To guide the development of optimal catalysts, the oxidation mechanisms of the fuels have to be fully understood. The oxidation of formic acid to CO₂, involving the exchange of only two electrons and the cleavage of a single C-H bond, is probably the simplest among the considered processes.^{1,2} In order to activate the aforementioned C-H bond cleavage, platinum surfaces are particularly effective, giving rise to overpotentials lower than those observed in the oxidation of small organic molecules on others metals. However, even on pure platinum, the measured oxidation currents, at low overpotentials, are still low. To increase the activity of the catalyst, modifications of platinum with other elements have been proposed. Intermetallic PtBi nanoparticles have shown an excellent performance, where high currents at very low overpotentials have been recorded.³⁻⁶ Nevertheless, the role played by Bi, or any other modifier, in the considered oxidation process is still unknown. In this work, using a combination of DFT calculations and experimental results on single crystal electrodes, the electro-oxidation mechanism of formic acid on the Bi-adatom modified Pt(111) surface is completely elucidated. Note that single crystal electrodes allow direct comparison between computational and experimental results.

The electrooxidation of formic acid on pure platinum electrodes can evolve following two main routes: through CO, which remains strongly adsorbed on the electrode, being difficult to oxidize, and through an active intermediate, which is the desired route.^{2,7} For this route, the nature of the intermediate is still under discussion.⁸⁻¹³ Electrocatalytic reactions rates depend on the surface structure of the electrodes. So, Pt(111) electrodes exhibit low activity through the active intermediate and negligible CO formation, whereas Pt(100) surfaces show the highest activity for both routes.^{14,15} Moreover, to increase the reaction rate through the direct route, pure platinum electrodes have been modified incorporating other species. Bismuth has given rise to very promising results.¹⁶⁻¹⁸ The addition of Bi adatoms to pristine Pt(111) single crystal electrodes diminishes the overpotentials and increase the current density up to 30-40 times that measured for the unmodified surface.¹⁵ Such improvement is clearly related to the deposition of Bi on the terraces, since it reaches the maximum for coverages close to the saturation value. For low and moderate Bi coverages, only isolated or <1 nm islands have been seen by STM, which supports the random distribution model of adatoms on the surface.¹⁹ Also, statistical models suggest that a Bi-Pt ensemble would be the reactive site, although the role played by each atom in the considered oxidation process has not yet been described.²⁰

It has been pointed out that, in the oxidation process of formic acid on pure platinum electrodes, adsorbed formate plays an important role. This specie has been detected by FTIR⁹⁻¹³ and voltammetry,²¹ coinciding the onset for the oxidation process with that for the adsorption of formate.²¹ Also, DFT calculations indicate that adsorbed formate is a key element in the considered oxidation process.^{22,23} More specifically, it has been suggested that adsorbed formate facilitates the adsorption of a new formic acid (or formate) molecule with the C-H bond directed towards the surface.²⁴ From such a configuration, the activation energy for the cleavage of the C-H bond would be low (ca. 0.5 eV), yielding CO₂ as final product. To adsorb the formate-formic dimer, a Pt ensemble with several Pt atoms is required. Thus, the initial hypothesis could be that bismuth facilitates the adsorption of formate on Pt sites.

To detect adsorption of formate on single crystal electrodes, fast scan voltammetry can be used.²¹ During formic acid oxidation, voltammetric currents come from two different processes: the oxidation process itself and adsorption processes (mainly hydrogen and anions) on the electrode surface. At low scan rates, oxidation currents are much higher than adsorption currents. However, adsorption currents are proportional to the scan rate, being oxidation currents much less affected by the scan rate.¹⁸ By using high scan rates, adsorption currents can dominate the voltammetric profile.²¹ For a Bi adatom modified Pt(111) electrode with a coverage of 0.25, which is very close to the maximum activity, both types of experiments (low and high scan rate voltammetry) are shown in figure 1. The same kind of experimental results are shown in figures S1-3 for the bare electrode and two additional coverages. As can be seen by comparison of the voltammograms in presence and absence of formic acid, at 50 mV s⁻¹ (figure 1A) adsorption currents are much smaller than those corresponding to formic acid oxidation, having the voltammogram the shape of an irreversible oxidation process, which is inhibited at high potentials. At high bismuth coverages and above 0.5 V, the incoming molecules are immediately oxidized on the electrode.

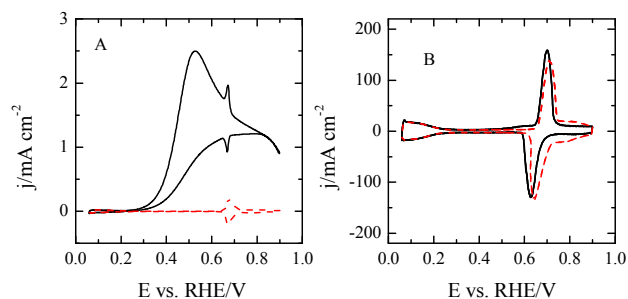


Figure 1. Voltammetric profiles of Bi-Pt(111) electrode with $\theta_{\text{Bi}}=0.25$ in 0.5 M HClO₄ + 0.05 M HCOOH (full line) and 0.5 M HClO₄ (dashed lines) at (A) 0.05 V s⁻¹ and (B) 50 V s⁻¹.

However, at 50 V s⁻¹ (Figure 1B and S1-3B) adsorption currents have increased 3 orders of magnitude, being the dominant process recorded in the voltammetry. In presence of formic acid voltammograms are practically symmetrical through the potential axis, which indicates that currents are mainly due to adsorption processes and thus, contribution from oxidation processes can be discarded. The comparison with the voltammograms measured in absence of formic acid enables to establish the formate adsorption range on platinum. In perchloric acid solutions, a hydrogen adsorption region appears at potentials below 0.3 V, whereas bismuth redox give rise to a pair of peaks between 0.6-0.7 V, in a similar way to what is found at 50 mV s⁻¹ (figure 1B and S4). Above 0.7 V, the signals corresponding to OH adsorption on Pt sites can be detected. In presence of formic acid at 50 V s⁻¹, some changes can be observed in the voltammograms. First, depending on the coverage, a signal corresponding to formate adsorption can be seen between 0.4-0.6 V in the positive scan direction (figure S5). In figure 1B, since bismuth coverage is high, the amount of free Pt sites is small, and therefore, the total amount of adsorbed formate on platinum is also small. However, in figure S5 the signal corresponding to formate adsorption diminishes as the coverage increases. For bismuth modified surfaces, the voltammograms in pres-

ence of formic acid at 50 V s⁻¹ are almost identical to those measured in sulfuric acid solutions in absence of formic acid, which corroborates that these processes are due to the adsorption of the formate anion.²⁵ As the amount of bismuth coverage increases, the onset for the formate anion adsorption is displaced towards higher potential values (see figure S5).²⁶ In parallel to the appearance of the new signal between 0.4 and 0.6 V, those corresponding to the adsorption of OH above 0.7 V disappear and a small shift in the bismuth redox peaks is observed. All these results indicate that for $\theta_{\text{Bi}}=0.25$ formate is present on platinum sites only above 0.5 V, whereas on the unmodified Pt(111) electrode it can be detected at 0.35 V.²¹ On the other hand, the onset potential for formic acid oxidation diminishes as the bismuth coverage increases. Thus, it is clear that the catalytic effect of bismuth is not linked to the adsorption of formate on Pt sites.

In order to gain insight into the mechanisms explaining the higher performance of bismuth modified electrodes, DFT calculations, modeling different aspects of the investigated process, were carried out. Adsorption of bismuth on fcc and hcp sites of the Pt(111) surface was found to be favorable by 3.20 eV and 3.17 eV, respectively. The adsorption of bismuth originates a redistribution of electron density on the bare surface. The results corresponding to fcc sites are displayed in figure 2, being the ones corresponding to hcp sites virtually identical. From figure 2, it can be inferred that an excess of positive charge would be concentrated on the adatom meanwhile the compensating negative charge would be distributed among the platinum atoms close to the adatom. Thus, bismuth has cationic character when adsorbed on Pt(111). Here we propose that the formation of the identified cationic site determines the oxidation process of formic acid on the Bi-Pt(111) surface driving its mechanism.

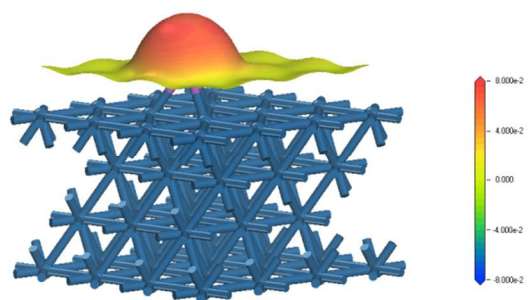


Figure 2. Electrostatic potential [Ha/e] mapped on electron iso-density surface for a density value $\rho = 0.01 \text{ e}/\text{\AA}^3$ for a Bi adatom adsorbed on the Pt(111) surface.

It was found that physisorption of hydrated formic acid near the adatom is favorable by ca. 0.26 eV. In its lower energy configuration, the carbonyl group is directed towards the adatom (figure S6), with changes in the bonds geometry being observed. In such a configuration, the O-H distance of the carboxylic group increases, whereas the distance to the corresponding hydrogen bond diminishes as compared to the distances calculated in absence of surface. Adatoms favoring physisorption of formic acid in the C-H down configuration has been previously found,²⁷ though the evolution of formic acid on the adatom site was not studied, and only the generic argument that that configuration facilitates the cleavage of the C-H bond, is provided. Here, the relevant role

played by the adatom during the oxidation process is established, and the complete oxidation mechanism is revealed.

From the described physisorbed configuration, the deprotonation of the formic acid molecule would be assisted by the fact that, from this location, formate was found to be favorably chemisorbed by 0.39 eV on the bismuth adatom without barrier. Therefore, formic acid deprotonation and formate chemisorption on bismuth would be two processes that would take place simultaneously. The above described physisorption and formate chemisorption related observations suggest that the pK_a of formic acid near the surface would be lower than that in the bulk. Physisorption, deprotonation, and formate chemisorption would be, all of them, processes driven by the positive charge located on the adatom.

Once formate chemisorption on the adatom has taken place, it was assumed that the electron in excess exits towards the circuit. So, the evolution of the HCOO fragment bonded to the bismuth modified platinum surface was analyzed. Running quantum mechanical molecular dynamics simulations, it was found that, transiting among different configurations whose energies fluctuate within the error of the calculations, the chemisorbed HCOO fragment evolves, in a rotating process for which the Bi-O and O-C bonds play the role of rotation axis, until a C-H down configuration sufficiently favorable is reached. From this configuration the C-H bond is cleaved to yield CO_2 and an adsorbed H atom (figure 3). The activation energy estimated from the calculations for the C-H bond cleavage step was negligible, presenting a favorable energy of 1.21 eV. Comparison with previous results on unmodified Pt(111) electrodes²⁴ shows a significant diminution in activation energy for the C-H bond cleavage step, from 0.5 to 0 eV.

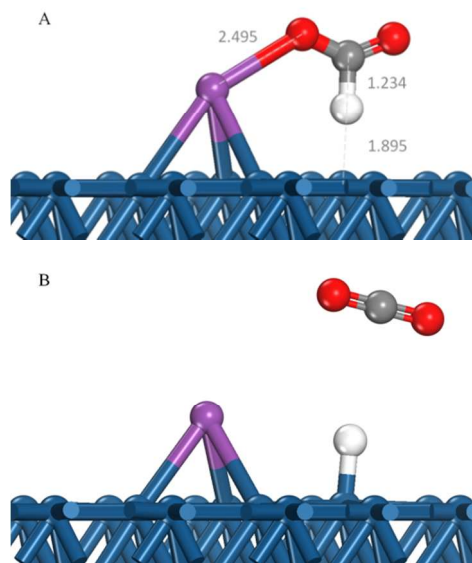


Figure 3. A) HCOO fragment adsorbed on the Bi-Pt(111) surface and B) final products in the oxidation of formic acid.

In summary, the here proposed model of oxidation reaction draws a bifunctional catalyst in which the bismuth adatom plays a determinant role in the formic acid adsorption and evolution to chemisorbed formate, whereas an adjacent Pt site is responsible for the cleavage of the C-H bond, which is in agreement with previous analysis suggesting that the catalytic site is a Bi-Pt ensemble.²⁰

To corroborate the proposed reaction mechanism, activation energies for different bismuth coverages on Pt(111) electrodes were experimentally estimated. For that, voltammetric profiles for the oxidation process were recorded at different temperatures (figure 4A). Since CO formation on these electrodes is negligible,^{15,17} the measured currents corresponds to the direct route. So, the logarithm of the current density at constant potential can be charted vs. T^{-1} in an Arrhenius plot to determine the apparent activation energy (figure S7). Activation energies vs. electrode potentials for different bismuth coverages are displayed in figure 4B. For comparison, the activation energy for the unmodified Pt(111) electrode is also included. For the bare electrode, the activation energy was determined from the intrinsic activity of the electrode through the active intermediate reaction measured at different temperatures.^{14,15}

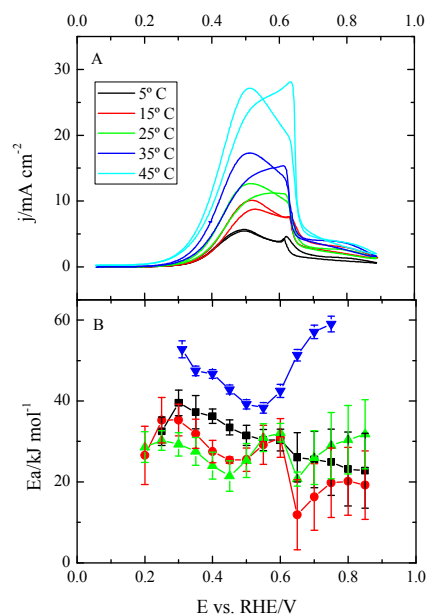


Figure 4. (A) Voltammetric profile of a Bi-Pt(111) electrode with $\theta_{Bi}=0.25$ in 0.5 M H_2SO_4 + 0.1 M $HCOOH$ at $0.05 V s^{-1}$ at different temperatures. (B) Measured activation energy for different Bi coverages (\blacktriangledown) $\theta_{Bi}=0.00$; (\blacksquare) $\theta_{Bi}=0.10$; (\bullet) $\theta_{Bi}=0.22$ and (\blacktriangle) $\theta_{Bi}=0.28$.

In figure 4B, as bismuth coverage increases, a significant diminution in the activation energy of the process can be observed. For the electrode with the highest activity, the diminution is around $20 kJ mol^{-1}$ with respect to that corresponding to the unmodified Pt(111) electrode. It should be borne in mind that experimentally estimated activation energies are apparent activation energies, which are a combination of the activation energies of all the different steps involved in a mechanism, whereas computationally estimated activation energies corresponds to a single step in a process. Additionally, in the case of the bismuth modified Pt(111) electrodes, the measured activation energy is an average of the activation energies for all the different kinds of reactive sites on the surface. For the investigated surfaces, two different kinds of active sites are considered: the Pt-Bi ensemble of figure 3, and the Pt ensemble on which the reaction occurs through the formate-formic dimer. If the activation energy for the Pt-Bi ensemble is much lower than that for the Pt sites, it is clear that the measured activation energy should

1
2
3
4
5
6
7
8
9
10
11
12
13
14
15
16
17
18
19
20
21
22
23
24
25
26
27
28
29
30
31
32
33
34
35
36
37
38
39
40
41
42
43
44
45
46
47
48
49
50
51
52
53
54
55
56
57
58
59
60

diminish when increasing bismuth coverage, as found experimentally. For the bismuth coverage with the highest catalytic activity ($\theta_{\text{Bi}}=0.28$), the measured activation energy is not zero because of the contribution of other previous steps and also from some Pt ensembles still accessible on the surface. At 0.45 V, the measured activation energy for $\theta_{\text{Bi}}=0.28$ is 21 kJ mol⁻¹, whereas on the unmodified surface is 42 kJ mol⁻¹. From these data, the contribution of the different steps/processes, to the apparent activation energy at this bismuth coverage, can be estimated. Since each bismuth adatom blocks 3 platinum sites, at the considered coverage, the number of free Pt sites is 0.16. This implies that the contribution of these sites to the total energy would be $0.16 \times 42 = 6.7$ kJ mol⁻¹. The remaining 14.3 kJ mol⁻¹ (or 0.15 eV) should arise, then, from the previous steps for the reaction on the Bi-Pt ensemble, probably from the deprotonation of the formic acid close to the Bi adatom to give rise to formate, which will adsorb immediately on the Bi adatom.

Finally, it should be stressed that the reaction mechanism suggested by our DFT calculations is in very good agreement with a broad set of experimental data. First, unlike the Pt(111) electrodes, for which currents increase with the pH,¹² the currents measured on the bismuth modified Pt(111) electrodes do not depend on the pH for values between 0 and 2,¹⁸ which implies that the formic acid molecule is the reactant species at these pH values. As has been shown, a formic acid molecule close to the Bi adatom would have a lower pK_a, which would facilitate its adsorption as formate on the bismuth adatom, and therefore, the presence of a formate molecule close to the adatom is not required. Second, the activation energy diminishes with the bismuth coverage. Third, the proposed reaction mechanism helps to explain why the onset of the reaction is between 0.2-0.3 V for the different bismuth coverages. In the final step, adsorbed hydrogen is formed, "poisoning" the active site. In order to reactivate the active site, hydrogen should be desorbed. Thus, a steady current for formic acid oxidation is only possible at potentials at which hydrogen is easily desorbed from the Pt sites, that is, where hydrogen equilibrium coverage on the surface is low. On the unmodified Pt(111) surface hydrogen coverage is low above 0.30 V, and this potential value diminishes as the bismuth coverage increases (see figure S4). Thus, the onset potential for the reaction shifts accordingly. And, fourth, the proposed mechanism also explain why the activation energy diminishes from 0.2 to 0.5 V. Hydrogen desorption also contributes to the measured activation energy, since it can be considered also the first step in the reaction at potentials where hydrogen is adsorbed. As the potential is made more positive, this step is faster (i.e., with a lower activation energy) which results in a diminution of the overall activation energy. As a conclusion, it can be verified that the here presented computational results are in very good agreement with a broad set of experimental data, explaining them, which fact rigorously support the proposed reaction model.

ASSOCIATED CONTENT

Supporting Information

Experimental details, computational methods and additional figures. This information is available free of charge via the Internet at //pubs.acs.org.

AUTHOR INFORMATION

Corresponding Author

herrero@ua.es

Notes

The authors declare no competing financial interests.

ACKNOWLEDGMENT

This work has been financially supported by the MINECO (Spain) (project CTQ2013-44083-P) and Generalitat Valenciana (project PROMETEOII/2014/013).

REFERENCES

- (1) Parsons, R.; Vandernoot, T. J. *Electroanal. Chem.* 1988, 257, 9.
- (2) Koper, M. T. M.; Lai, S. C. S.; Herrero, E. In *Fuel cell catalysis, a surface science approach*; Koper, M. T. M., Ed.; John Wiley & Sons, Inc: Hoboken, NJ, 2009, p 159.
- (3) Roychowdhury, C.; Matsumoto, F.; Zeldovich, V. B.; Warren, S. C.; Mutolo, P. F.; Ballesteros, M.; Wiesner, U.; Abruna, H. D.; DiSalvo, F. J. *Chem. Mater.* 2006, 18, 3365.
- (4) Roychowdhury, C.; Matsumoto, F.; Mutolo, P. F.; Abruna, H. D.; DiSalvo, F. J. *Chem. Mater.* 2005, 17, 5871.
- (5) Casado-Rivera, E.; Gal, Z.; Angelo, A. C. D.; Lind, C.; DiSalvo, F. J.; Abruna, H. D. *ChemPhysChem* 2003, 4, 193.
- (6) Blasini, D. R.; Rochefort, D.; Fachini, E.; Alden, L. R.; DiSalvo, F. J.; Cabrera, C. R.; Abruna, H. D. *Surf. Sci.* 2006, 600, 2670.
- (7) Feliu, J. M.; Herrero, E. In *Handbook of fuel cells - fundamentals, technology and applications*; Vielstich, W., Gasteiger, H., Lamm, A., Eds.; John Wiley & Sons, Ltd.: Chichester, 2003; Vol. 2.
- (8) Samjeske, G.; Miki, A.; Ye, S.; Osawa, M. *J. Phys. Chem. B* 2006, 110, 16559.
- (9) Chen, Y. X.; Ye, S.; Heinen, M.; Jusys, Z.; Osawa, M.; Behm, R. J. *J. Phys. Chem. B* 2006, 110, 9534.
- (10) Cuesta, A.; Cabello, G.; Gutierrez, C.; Osawa, M. *Phys. Chem. Chem. Phys.* 2011, 13, 20091.
- (11) Osawa, M.; Komatsu, K.; Samjeske, G.; Uchida, T.; Ikeshoji, T.; Cuesta, A.; Gutierrez, C. *Angew. Chem. Int. Edit.* 2011, 50, 1159.
- (12) Joo, J.; Uchida, T.; Cuesta, A.; Koper, M. T. M.; Osawa, M. *J. Am. Chem. Soc.* 2013, 135, 9991.
- (13) Chen, Y. X.; Heinen, M.; Jusys, Z.; Behm, R. J. *Langmuir* 2006, 22, 10399.
- (14) Grozovski, V.; Climent, V.; Herrero, E.; Feliu, J. M. *ChemPhysChem* 2009, 10, 1922.
- (15) Grozovski, V.; Climent, V.; Herrero, E.; Feliu, J. M. *Phys. Chem. Chem. Phys.* 2010, 12, 8822.
- (16) Clavilier, J.; Fernández-Vega, A.; Feliu, J. M.; Aldaz, A. J. *Electroanal. Chem.* 1989, 258, 89.
- (17) Herrero, E.; Fernández-Vega, A.; Feliu, J. M.; Aldaz, A. J. *Electroanal. Chem.* 1993, 350, 73.
- (18) Maciá, M. D.; Herrero, E.; Feliu, J. M. *J. Electroanal. Chem.* 2003, 554, 25.
- (19) Kim, J.; Rhee, C. K. *Electrochem. Commun.* 2010, 12, 1731.
- (20) Leiva, E.; Iwasita, T.; Herrero, E.; Feliu, J. M. *Langmuir* 1997, 13, 6287.
- (21) Grozovski, V.; Vidal-Iglesias, F. J.; Herrero, E.; Feliu, J. M. *ChemPhysChem* 2011, 12, 1641.
- (22) Neurock, M.; Janik, M.; Wieckowski, A. *Faraday Discuss.* 2009, 140, 363.
- (23) Gao, W.; Keith, J. A.; Anton, J.; Jacob, T. J. *Am. Chem. Soc.* 2010, 132, 18377.
- (24) Wang, H.-F.; Liu, Z.-P. *J. Phys. Chem. C* 2009, 113, 17502.
- (25) Clavilier, J.; Feliu, J. M.; Aldaz, A. J. *Electroanal. Chem.* 1988, 243, 419.
- (26) Climent, V.; Herrero, E.; Feliu, J. M. *Electrochem. Commun.* 2001, 3, 590.
- (27) Peng, B.; Wang, H.-F.; Liu, Z.-P.; Cai, W.-B. *J. Phys. Chem. C* 2010, 114, 3102.

1
2
3
4
5
6
7
8
9
10
11
12
13
14
15
16
17
18
19
20
21
22
23
24
25
26
27
28
29
30
31
32
33
34
35
36
37
38
39
40
41
42
43
44
45
46
47
48
49
50
51
52
53
54
55
56
57
58
59
60

Insert Table of Contents artwork here

